



**HAL**  
open science

## Temporal evolution of plastic additive contents over the last decades in two major European rivers (Rhone and Rhine) from sediment cores analyses

Alice Vidal, Laure Papillon, Gabrielle Seignemartin, Amandine Morereau, Cassandra Euzen, Christian Grenz, Yoann Copard, Frédérique Eyrolle, Richard Sempere

### ► To cite this version:

Alice Vidal, Laure Papillon, Gabrielle Seignemartin, Amandine Morereau, Cassandra Euzen, et al.. Temporal evolution of plastic additive contents over the last decades in two major European rivers (Rhone and Rhine) from sediment cores analyses. 2024. hal-04570244

**HAL Id: hal-04570244**

**<https://amu.hal.science/hal-04570244>**

Preprint submitted on 6 May 2024

**HAL** is a multi-disciplinary open access archive for the deposit and dissemination of scientific research documents, whether they are published or not. The documents may come from teaching and research institutions in France or abroad, or from public or private research centers.

L'archive ouverte pluridisciplinaire **HAL**, est destinée au dépôt et à la diffusion de documents scientifiques de niveau recherche, publiés ou non, émanant des établissements d'enseignement et de recherche français ou étrangers, des laboratoires publics ou privés.

# Journal Pre-proof

Temporal evolution of plastic additive contents over the last decades in two major European rivers (Rhône and Rhine) from sediment cores analyses

Alice Vidal, Laure Papillon, Gabrielle Seignemartin, Amandine Morereau, Cassandra Euzen, Christian Grenz, Yoann Copard, Frédérique Eyrolle, Richard Sempéré



PII: S0269-7491(24)00369-5

DOI: <https://doi.org/10.1016/j.envpol.2024.123655>

Reference: ENPO 123655

To appear in: *Environmental Pollution*

Received Date: 24 November 2023

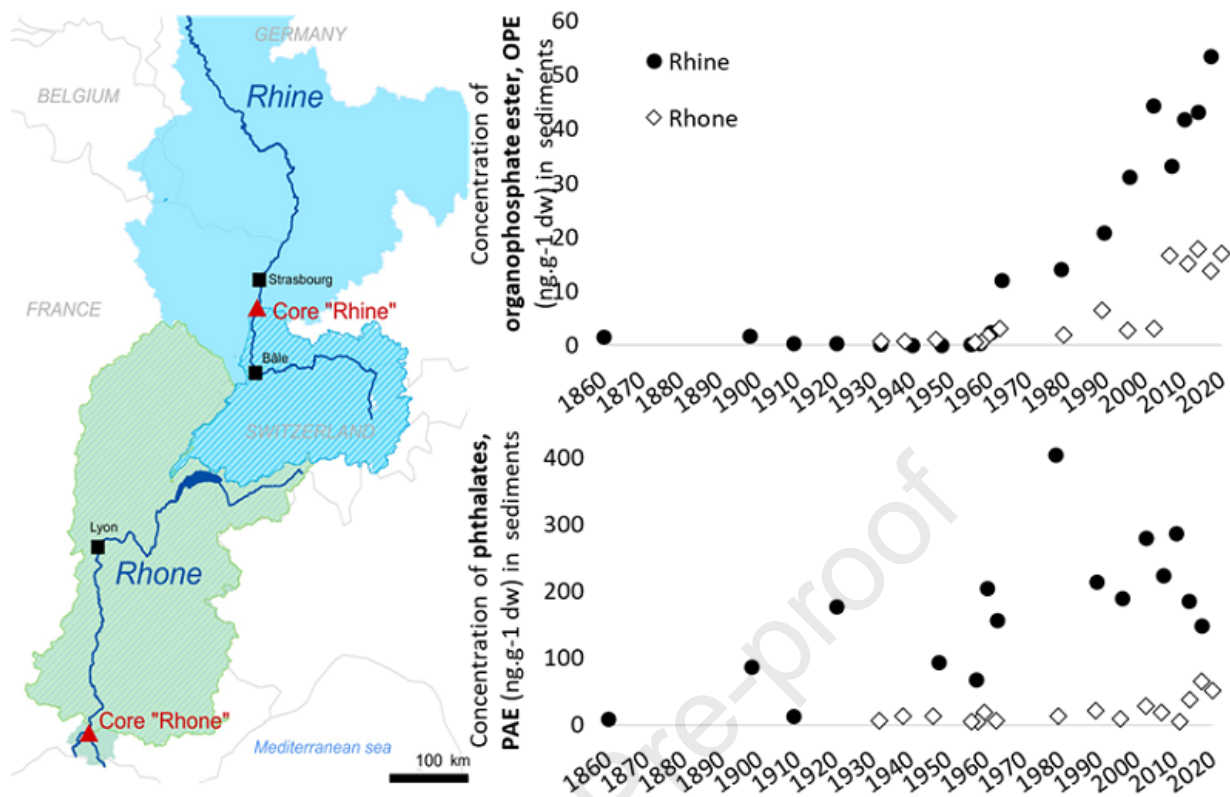
Revised Date: 22 February 2024

Accepted Date: 23 February 2024

Please cite this article as: Vidal, A., Papillon, L., Seignemartin, G., Morereau, A., Euzen, C., Grenz, C., Copard, Y., Eyrolle, Frée., Sempéré, R., Temporal evolution of plastic additive contents over the last decades in two major European rivers (Rhône and Rhine) from sediment cores analyses, *Environmental Pollution* (2024), doi: <https://doi.org/10.1016/j.envpol.2024.123655>.

This is a PDF file of an article that has undergone enhancements after acceptance, such as the addition of a cover page and metadata, and formatting for readability, but it is not yet the definitive version of record. This version will undergo additional copyediting, typesetting and review before it is published in its final form, but we are providing this version to give early visibility of the article. Please note that, during the production process, errors may be discovered which could affect the content, and all legal disclaimers that apply to the journal pertain.

© 2024 Published by Elsevier Ltd.



# Temporal evolution of plastic additive contents over the last decades in two major European rivers (Rhône and Rhine) from sediment cores analyses.

Alice Vidal<sup>1</sup>, Laure Papillon<sup>1</sup>, Gabrielle Seignemartin<sup>2</sup>, Amandine Morereau<sup>3,4</sup>, Cassandra Euzen<sup>5</sup>, Christian Grenz<sup>1</sup>, Yoann Copard<sup>6</sup>, Frédérique Eyrolle<sup>3</sup>, Richard Sempéré<sup>1</sup>

<sup>1</sup> Aix-Marseille Univ., Toulon University, CNRS, IRD, UM 110, Marseille, France

<sup>2</sup> Univ. Lyon, Université Claude Bernard Lyon 1, CNRS, ENTPE, UMR5023 LEHNA, F-69518, Vaulx-en-Velin, France

<sup>3</sup> Institut de Radioprotection et de Sûreté Nucléaire (IRSN), PSE-ENV, STAAR/LRTA, BP 3, 13115 Saint-Paul-lez-Durance, France

<sup>4</sup> Sorbonne-Université, UMR CNRS 7619 METIS, 75252 Paris, France

<sup>5</sup> Univ. Strasbourg, CNRS, ENGEES, UMR7362 LIVE, Strasbourg, France

<sup>6</sup> Univ. Rouen Normandie, Université Caen Normandie, CNRS, Normandie Univ, M2C UMR 6143, F-76000 Rouen, France

## Abstract

Although global plastic distribution is at the heart of 21<sup>st</sup> century environmental concerns, little information is available concerning how organic plastic additives contaminate freshwater sediments, which are often subject to strong anthropogenic pressure. Here, sediment core samples were collected in the Rhône and the Rhine watersheds (France), dated using <sup>137</sup>Cs and <sup>210</sup>Pb<sub>xs</sub> methods and analysed for nine phthalates (PAEs) and seven organophosphate esters (OPEs). The distribution of these organic contaminants was used to establish a chronological archive of plastic additive pollution from 1860 (Rhine) and 1930 (Rhône) until today. Sediment grain size and parameters related to organic matter (OM) were also measured as potential factors that may affect the temporal distribution of OPEs and PAEs in sediments. Our results show that OPE and PAE levels increased continuously in Rhône and Rhine sediments since the first records. In both rivers,  $\Sigma$ PAEs levels (from 9.1±1.7 to 487.3±27.0 ng.g<sup>-1</sup> dry weight (dw) ± standard deviation and from 4.6±1.3 to 65.2±11.2 ng.g<sup>-1</sup> dw, for the Rhine and the Rhône rivers, respectively) were higher than  $\Sigma$ OPEs levels (from 0.1±0.1 to 79.1±13.7 ng.g<sup>-1</sup> dw and from 0.6±0.1 to 17.8±2.3 ng.g<sup>-1</sup> dw, for Rhine and Rhône rivers, respectively). In both rivers, di(2-ethylhexyl) phthalate (DEHP) was the most abundant PAE, followed by diisobutyl phthalate (DiBP), while tris (2-chloroisopropyl) phosphate (TCPP) was the most abundant OPE. No relationship was found between granulometry and additives concentrations, while organic matter helps explain the vertical distribution of PAEs and OPEs in the sediment cores. This study thus establishes a temporal trajectory of PAEs and OPEs contents over the last decades, leading to a better understanding of historical pollution in these two Western European rivers.

**Keywords:** Organic plastic additives; Phthalates; Organophosphate esters; River sedimentary archives; Contamination trajectories; Historical pollution

**Abbreviations:** Tripropyl phosphate (TPP); Tri-iso-butyl phosphate (TiBP); Tributyl-n-phosphate (TnBP); Tris-(2-chloroethyl) phosphate (TCEP); Tris(2-chloro-1-methylethyl) phosphate (TCPP); Tris(chloroisopropyl) phosphate (TCPP-1); Bis(2-chloro-1-methylethyl)(2-chloropropyl) phosphate (TCPP-

40 2); Triphenyl phosphate (TPhP); 2-ethylhexyl diphenyl phosphate (EHDPP); Tri(2-ethylhexyl) phosphate  
41 (TEHP); Tris (1,3-dichloro-2-propyl) phosphate (TDCP); Tripropyl phosphate (TPrP); Tricresyl phosphate  
42 (TCrP); Tris (1,3-dichloro-2-propyl) phosphate (TDCPP); Tris (2-butoxyethyl) phosphate (TBEP); Diethyl  
43 phthalate (DEP); Di(2-ethylhexyl) phthalate (DEHP); Di-n-butyl phthalate (DnBP); Dimethylphthalate  
44 (DMP); Diisobutyl phthalate (DiBP); Benzyle butyle phthalate (BBzP); Di-n-octyl phthalate (DnOP).

45

Journal Pre-proof

## 1. Introduction

Over the last decades, plastic pollution has become a major environmental concern due to its increasing production which was estimated at 390.7 million metric tons in 2021 (Statista Research Department, 2023). Plastics play an important role in the Anthropocene with many being used only once and immediately discarded, most frequently inappropriately. Some of them reach the terrestrial environment and ultimately end up in aquatic environments. Once they reach the aquatic compartment, plastics will be fragmented into smaller sized particles by photodegradation (UV radiation), weathering and physical abrasion (e.g., wind and wave action), as well as by biotic factors (e.g., microorganisms action). Since the beginning of plastic production, a panel of additives have been added to polymers by manufacturers so as to confer particular properties to plastic polymers. Among the organic additives, phthalates (PAEs) and organophosphate esters (OPEs) are the most abundant (Yang et al., 2019). For example, PAEs are used as plasticizers to facilitate processing and to increase the flexibility and the toughness of manufactured plastic products, while OPEs serve as flame retardants and plasticizers (Wang et al., 2020). These chemicals are also added to paints, adhesives, cosmetics and personal care products (Guo and Kannan, 2012; Cao, 2010), and are subsequently released into the surrounding environment as the products age (Paluselli et al., 2018; Fauvelle et al., 2021). In recent years, studies have highlighted the ecotoxicological concerns of these chemicals for living aquatic organisms (Net et al., 2015; Wei et al., 2015). During riverine transport of organic matter including both natural and anthropogenic compounds, the physicochemical properties of a myriad of hydrophobic compounds leads them to bind with carbon-rich suspended particulate matter (van der Veen and de Boer, 2012; Net et al., 2015), which then accumulate in the sediment throughout watersheds and in coastal areas (Schmidt et al., 2018; Paluselli et al., 2018). Sedimentary archives from large rivers have been widely explored in recent years (Foucher et al., 2021), and are expected to trace the history of the chemicals introduced by the technological and industrial activities which define the 20<sup>th</sup> century. However, river sediment cores remain poorly studied for plastics and their additives.

In France, the Rhone and the Rhine are two major rivers most impacted by human activities. They have been strongly modified by the construction of dams, by wastewater treatment plant inputs and by hydro-electrical facilities. Both rivers have previously been studied mainly for the most common heavy metals (e.g. zinc, lead, cadmium, copper) and organic pollutants (e.g. perfluoroalkyl substances, polychlorinated biphenyls, polycyclic aromatic hydrocarbons) (Middelkoop, 2000; Heise and Förstner, 2006; Mourier et al., 2014; Munoz et al., 2015; Mourier et al., 2019; Dendievel et al. 2020; Joerss et al. 2020; Schmidt et al., 2020). More recently, studies reported the presence of plastic additives in freshwater ecosystems. In the sediments of the Rhone River, Alkans et al. (2021) averaged OPE and PAE levels, at  $24.9 \pm 6.0 \text{ ng.g}^{-1}$  dry weight (dw) and  $69.0 \pm 17.4 \text{ ng.g}^{-1}$  dw, respectively. Paluselli et al. (2017) averaged the PAE concentration in the Rhone River surface water at  $615.1 \text{ ng.L}^{-1}$ . To the best of our knowledge, the occurrence of OPEs

81 remains unmeasured in the Rhine River, and only Nagorka and Koschorreck (2020) have reported data on  
82 PAEs in suspended particulate matter from the Rhine River ( $>2000 \text{ ng.g}^{-1}$ ). Furthermore, knowledge of  
83 historical contamination trends of OPEs and PAEs in riverine sediments remains poor, because few studies  
84 precisely date the sediment cores which leads to potential biases regarding the period of time associated  
85 with measurements. Understanding the historical trajectories of organic plastic additives in sediment  
86 cores is of great importance for estimating the inventory of contaminants that can be associated in part  
87 to plastic debris items transferred by rivers to oceans, and for evaluating their impacts on the environment  
88 over time. In this context, our study aims to establish the temporal trends of the concentrations of  
89 common plastic additives including seven PAEs and nine OPEs by examining dated Rhone and Rhine  
90 sediment cores collected at the outlets of watersheds since the beginning of the last century. The grain  
91 size distribution as well as organic matter parameters were measured to establish relationships between  
92 these key factors and the distribution of OPE and PAE concentrations in the sediments over one century.  
93 These results contribute to a better understanding of the plastic additive contamination of freshwater  
94 streams, and provide data to implement public policies for environmental risk management.

## 95 **2. Materials and Methods**

### 96 **2.1. Study sites**

97 Sediment core samples were selected in the downstream section of the Rhone and the Rhine  
98 rivers in France (Figure 1) using historical maps, aerial photographs, and both bibliographic and field  
99 investigations. Documentary supports allowed to determine as far as was possible, those areas where  
100 sedimentary deposition has occurred continuously over the past decades.

101 The Rhone River stretches for 812 km, originating at the Furka Glacier (2340 m asl) in the Swiss Alps and  
102 spanning a 98,500 km<sup>2</sup> watershed with a complex hydrological regime (Olivier et al., 2009). The river flows  
103 into the Mediterranean Sea, with an average annual discharge of 1,700 m<sup>3</sup>.s<sup>-1</sup> (Olivier et al., 2022) and is  
104 the main provider of terrestrial inorganic and organic carbon to the Mediterranean (Sempéré et al., 2000).  
105 Throughout the latter half of the 20<sup>th</sup> century, numerous dams were constructed along the river to satisfy  
106 the need for hydroelectric power production, thus transforming the river into a single-thread channel  
107 (Tena et al., 2020; Riquier, 2015; Bravard, 2010). Originally initiated by the construction of dike fields and  
108 later reinforced by the installation of diversion dams, terrestrialization has led to the deposition of fine  
109 sediments, to alterations in water levels, and ultimately, to modifications in the hydrological connection  
110 at the margins (Seignemartin et al., 2023). These developments provide context to the Rhone core,  
111 revealing sediment deposition in the 1960s within a previously aquatic zone (Figure 1.B). The study site is  
112 situated just upstream of the delta and the city of Arles, at the south end of the Lower Rhone segment  
113 (Figure 1.A). Its associated drainage area covers 98% of the total watershed area (Figure 1.C).

114 The Rhine River, which extends for 1,233 km, originates in the Swiss Alps at Lake Tomasee. Its watershed  
115 covers 185,000 km<sup>2</sup> spanning nine European countries and has an average annual discharge of about

116 2,300 m<sup>3</sup>.s<sup>-1</sup> into the North Sea. The hydrological Rhine regime is nival and the mean annual discharge at  
117 the Basel gauging station is 1050 m<sup>3</sup>.s<sup>-1</sup>. During the mid-19<sup>th</sup> century, the upper Rhine underwent human  
118 modifications including channelization efforts for flood control, bank delineation, agricultural  
119 advancement, and forest expansion, while dams were constructed in the 20<sup>th</sup> century (Schmitt, 2001;  
120 Arnaud, 2015). The Rhine River core originates from the artificial island created by the diversion of the  
121 Rhinau dam, built in 1963, in a former braiding and anastomose area that became stabilised due to  
122 channelization (Figure 1.B). The drained area associated with the core covers about 20% of the total Rhine  
123 watershed, encompassing the entirety of its Swiss and French parts (Figures 1.A and 1.B).

## 124 **2.2. Sediment sampling and core dating**

125 Cores were sampled on 11/19/2020 and 03/09/2020 on the Rhone River and on the Rhine River,  
126 respectively. Rhone and Rhine cores were collected using a percussion driller (Cobra TT, SDEC, France)  
127 with transparent PVC tubes (diameter 46 mm or 100 mm). For the Rhone deposit, which is more than 1  
128 m thick, a master core was obtained by twice sampling successive 1-m sediment cores over less than 1 m<sup>2</sup>  
129 surface area. The second coring was vertically shifted by 50 cm compared to the first one in order to  
130 preserve sediment samplings from interface disruptions. Once in the laboratory, each 1 m core was cut  
131 lengthwise, and slices varying from one to several cm were successively sampled from the surface to the  
132 depth, depending on stratigraphy. Slices were stored at -25°C and freeze-dried under dehydrated  
133 nitrogen flux to avoid any atmospheric exchange, and were sieved at 2 mm before analyses.

134 Sedimentary core samples were analysed by gamma spectrometry. Dry samples were conditioned  
135 in 17- or 60-mL tightly closed plastic boxes for gamma counting using low-background and high-resolution  
136 Germanium Hyper pure detectors at the IRSN/LMRE laboratory in Orsay (Bouisset and Calmet, 1997). The  
137 boxes were placed in vacuum sealed packages and stored for at least one month before measurement to  
138 ensure the secular equilibrium of the <sup>210</sup>Pb necessary to determine the concentration of <sup>210</sup>Pb<sub>xs</sub> (<sup>210</sup>Pb in  
139 excess). Efficiency calibrations were constructed using gamma-ray sources in a 1.15 g/cm<sup>3</sup> density solid  
140 resin–water equivalent matrix. Activity results were corrected for true coincidence summing and self-  
141 absorption effects (Lefèvre et al., 2003). Measured activities, expressed in Bq.kg<sup>-1</sup> dry weight, were decay-  
142 corrected to the date of sampling. Activity uncertainty was estimated as the combination of calibration  
143 uncertainties, counting statistics, and summing and self-absorption correction uncertainties. A wide range  
144 of gamma emissions were detected with a germanium detector including <sup>137</sup>Cs, <sup>210</sup>Pb and <sup>214</sup>Bi used to  
145 determine <sup>210</sup>Pb<sub>xs</sub>. These latter are widely used to date recent sediment deposits (last 100 years) because  
146 their half-life allows to cover several decades: 30.08 years for <sup>137</sup>Cs and 22.20 years for <sup>210</sup>Pb (Goldberg,  
147 1963). Around 30% of sedimentary core samples were additionally analysed by alpha spectrometry after  
148 radiochemistry steps to quantify plutonium isotopes (<sup>238</sup>Pu, <sup>239,240</sup>Pu), <sup>241</sup>Am and <sup>244</sup>Cm. <sup>137</sup>Cs and other  
149 chronological tracers dating method (method A) and <sup>210</sup>Pb<sub>xs</sub> dating method (method B) were detailed in  
150 Section S1 (supplementary data), (Eyrolle et al., submitted).



### 151 **2.3. Sediment grain size distribution**

152 Particle size analyses were carried out on fresh sediment samples using a Beckman Coulter LS  
153 13320 laser micro-particle size analyser (measurement interval between 0.04 and 1,813  $\mu\text{m}$ ). Each  
154 measurement was carried out 3 times (triplicate samples) to reduce heterogeneity uncertainties within  
155 the samples, while the d50 and d90 were calculated for each sediment sample and the particle classes  
156 were determined according to the classification of Blott and Pye (2001) and processed using Gradistat  
157 (Blott, 2000): clay ( $x < 2 \mu\text{m}$ ), silt ( $2 \mu\text{m} < x < 63 \mu\text{m}$ ) and sand ( $x > 63 \mu\text{m}$ ).

### 158 **2.4. Organic matter parameters**

159 Sedimentary Organic Matter (OM) was characterised using classical bulk organic Rock-Eval 6  
160 pyrolysis (Copard et al., 2006; Baudin et al., 2015), providing total organic carbon (TOC) content and other  
161 OM indicators. Such analyses reveal (i) the amount of hydrogenous compounds contained in OM, (ii) the  
162 OI (oxygen index, in  $\text{mg O}_2\cdot\text{g}^{-1}$  TOC) corresponding to the amount of oxygenated compound contained in  
163 OM, (iii) the total organic carbon (TOC, in wt. %) corresponding to the sum of the carbon calculated from  
164 pyrolysis and oxidation (RC) steps, (iv) the RC/TOC ratio showing the refractory character of OM and (v)  
165 the HI/OI ratio derived from the pyrolysis signals (S2, S3, S3CO) which reveals the global origin and the  
166 degradation states of OM (Carrie et al., 2012). S2 (mg of hydrocarbon/g of sample), S3 (mg of  $\text{CO}_2$ /g of  
167 sample) and S3CO (mg of CO/g of sample) are time-integrated signals from pyrolysis step. S2 is referred  
168 to the release of hydrocarbon compounds during all the temperature programming. S3 and S3CO are  
169 respectively the release of  $\text{CO}_2$  and CO from the decomposition of sedimentary OM before  $400^\circ\text{C}$ .

### 170 **2.5. Extraction and analysis of OPEs and PAEs**

171 All information on chemical and reagent suppliers is detailed in the Table S1. Sediment samples  
172 were sieved through a pre-cleaned stainless-steel sieve (500  $\mu\text{m}$  diameter) before extraction. All sediment  
173 samples were treated with the procedure described by Alkan et al. (2021). Briefly, the sediments samples  
174 ( $3.00 \pm 0.05$  g dry weight (dw)) were mixed with active copper (1 g) and labelled surrogate standards (10  
175  $\mu\text{L}$  of TBP-d27, TCPP-d18, TDCP-d15, DnBP-d4 at  $10 \text{ ng}\cdot\text{mL}^{-1}$ ) to monitor the overall extraction efficiency  
176 of the target compounds. Cartridges (conditioned with acetone, EtOAc and DCM) containing  $250 \pm 2.5$  mg  
177 of Oasis MAX (Waters) sandwiched between two PTFE frits were mounted in a 12-port SPE vacuum  
178 Manifold (Supelco, Sigma-Aldrich) for the extraction, three of which corresponded to blanks for each  
179 extraction. Two extractions were undertaken: the first with DCM and the second with DCM/EtOAc  
180 (70/30). The combined extracts were evaporated to 1 mL under gentle flow using a 12-port Visidry Drying  
181 Attachment (Supelco, Sigma-Aldrich). An additional clean-up step was performed by passing the extracts  
182 through 3% deactivated alumina (1.5 g) packed in a pre-cleaned Pasteur pipette topped with 0.5 g of  
183 sodium sulphate. Finally, the new extract was evaporated (50  $\mu\text{L}$ ) into a GC vial. 100 ng of labelled OPE  
184 and PAE was added to each sample for the quantification of target compounds, and the extracts were  
185 stored at  $-20^\circ\text{C}$  until Gas Chromatography – tandem Mass Spectrometry (Triple Quadrupole) (GC-MS/MS)

186 (QQQ)) analysis (Agilent 8890 Series GC coupled with an Agilent 7000D TQ), operating in multiple reaction  
187 monitoring (MRM) and electron impact (EI, 70 eV) modes. The separation was achieved in a 30 m x 0.25  
188 mm i.d. x 0.25  $\mu\text{m}$  HP-5MS capillary column (Agilent J&W). All target contaminants were quantified  
189 according to the internal standard procedure. The injection volume was 2  $\mu\text{L}$  and the helium carrier gas  
190 flow was 1  $\text{mL}\cdot\text{min}^{-1}$ . The temperatures of the Mass Selective Detector transfer line and the ion source  
191 and quadrupole were set at 150°C. The following conditions were applied: injector temperature, 270°C  
192 (splitless) and the oven was programmed from 90°C to 166°C at 4°C $\cdot\text{min}^{-1}$ , to 175 at 3°C $\cdot\text{min}^{-1}$  (holding  
193 time 2 min), to 232°C at 4°C $\cdot\text{min}^{-1}$ , to 290°C at 10°C $\cdot\text{min}^{-1}$  and then to 310°C at 10°C $\cdot\text{min}^{-1}$  (holding time  
194 7.4 min). The total duration of one sample analysis was thus 53.45 min.

### 195 **2.6. Cross-contamination from the coring**

196 Additional analyses were performed to quantify the levels of OPEs and PAEs introduced by the  
197 PVC made-corer itself, despite the permanent and rigorous aspiration during the coring stage and the  
198 precautions taken during each of the treatment steps. An experimental blank sediment sample was  
199 therefore baked at 450°C for 6h to eliminate any potential trace of additives and was rewet with ultra-  
200 pure water. Blank sediment was introduced into the PVC-made corer and the same treatment was applied  
201 as for the experimental samples. Three replicates of blank sediment were collected at the end of the  
202 whole procedure. All replicates were then treated to extract the additives (OPEs and PAEs) and were  
203 analysed following the same methodology as for the experimental sediment samples. The cross-  
204 contamination was quantified for each PAE and each OPE (Table S2). Finally, to homogenize the results  
205 and allow a comparison between the two rivers, the given concentrations were first corrected by the  
206 recoveries, then blank concentrations and concentrations from cross-contamination were subtracted.

### 207 **2.7. Quality assurance/quality control**

208 Strict measures were taken to prevent potential cross contamination during OPE and PAE analysis.  
209 First, the use of plastic material was avoided at all times and all glassware was cleaned overnight with  
210 detergent, rinsed with tap water + MQ water and then baked at 450°C for 6 h before use. Alumina and  
211 sodium sulphate were also baked overnight at 450°C before use. Sample treatment and extraction/clean-  
212 up steps were performed entirely in an International Standards Organization (ISO) 6 cleanroom (22°C, SAS  
213 + 15 Pa cleanroom pressure, 50  $\text{vol}\cdot\text{h}^{-1}$  brewing rate) (Paluselli et al., 2018). The retention time and the  
214 response factors of GC-MS/MS (QQQ) were evaluated for each analytical sequence by regularly injecting  
215 different calibration levels. One hexane injection was performed every 3 samples to check and monitor  
216 potential cross contamination along the sequence. In addition, all samples analysed were spiked with  
217 labelled surrogates. The average recoveries and the mean blank values are presented in Table S3. All  
218 concentrations of PAE and OPE ( $\text{ng}\cdot\text{g}^{-1}$ ) presented in this study have been corrected by subtracting the  
219 corresponding mean blank value and the concentration introduced by the coring.

### 220 **2.8. Statistical analysis**

221 Pearson correlations were performed using data related to organic matter (TOC, RC/TOC, S2, S3,  
222 S3CO3 and HI/OI), granulometry (d10, d50 and d90), and PAE and OPE concentrations for Rhone and Rhine  
223 sediment samples in order to evaluate the relationships between the sediment grain size, OM, and plastic  
224 additive concentrations over time. Pearson correlation coefficients were performed with the Rstudio  
225 application associated with R software (version 4.3.1).

### 226 3. Results

#### 227 **3.1. Age/depth models based on $^{137}\text{Cs}$ and alpha emitters chronological tracers, and $^{210}\text{Pb}_{\text{xs}}$** 228 **profiles**

229 Our results show that along the Rhine sedimentary core,  $^{137}\text{Cs}$  mainly peaks at 21 cm depth (91.1  
230 Bq.kg<sup>-1</sup>) while all alpha emitters ( $^{238}\text{Pu}$ ,  $^{239,240}\text{Pu}$ ,  $^{241}\text{Am}$ ,  $^{244}\text{Cm}$ ) peak at around 27 cm (Figure S1). These  
231 maximums can be attributed to the years 1986 (Chernobyl accident) and 1963 (Atmospheric global fallout  
232 for nuclear tests), respectively, whereas the drastic  $^{137}\text{Cs}$  activity decrease towards detection limits below  
233 41 cm indicates that the pre-bomb test period was reached in 1955. The sandy strata at 75-80cm depth  
234 corresponds probably to extreme flood events after the beginning of the correction works (Euzen et al.,  
235 submitted). Additionally, Euzen et al. (submitted) reported an additional chronological benchmark at 80  
236 cm depth attributed to the year 1882. The use of all these chronological tracers gives calculated apparent  
237 sedimentation rates (ASR) of 0.5, 1.8, 0.3 and 0.6 cm.y<sup>-1</sup> for the 1882-1955, 1955-1963, 1963-1986 and  
238 1986-2021 periods, respectively, which is in line with estimations obtained using the  $^{210}\text{Pb}_{\text{xs}}$  approach  
239 (Table S4, Figures S1 and S2).

240 The Rhone core results show increasing  $^{137}\text{Cs}$  activities starting from 250.5 cm depth, which can  
241 be attributed to the 1955 nuclear events (Figure S1). Activities of  $^{137}\text{Cs}$  and artificial alpha emitters vary  
242 towards maximum values of between 139 and 233 cm, highlighting the releases from the spent fuel  
243 reprocessing plant. Those releases were the most important over the 1963-1990 period and partially mask  
244 the Chernobyl accident contribution (Eyrolle et al., 2008; Provansal et al., 2010). By using these  
245 chronological benchmarks, mean ASR are 3.8, 3.5 and 4.5 cm.y<sup>-1</sup> for the periods 1955-1963, 1963-1990  
246 and 1990-2020, respectively. These values are very close to those calculated over the 1930-2020 period  
247 using the  $^{210}\text{Pb}_{\text{xs}}$  method, i.e. 3.8 cm.y<sup>-1</sup> (Figure S1). A mean apparent sedimentation rate of 3.8 cm.y<sup>-1</sup> can  
248 therefore be extrapolated here for the pre-1955 period.

#### 249 **3.2. Grain-size sediment distribution**

250 Our results show that silts make up most of the sedimentary particles in both rivers, with an  
251 exception at around 260 cm depth in the Rhone core where sands are seen to dominate (Figure 2). These  
252 sedimentary layers, corresponding to the 1950s in the Rhone core, probably highlight one or several major  
253 flood events (flow rates in the range of 7760-9180 m<sup>3</sup>.s<sup>-1</sup>). Interestingly, the small but significant increase  
254 of amounts of sand around 15, 60 and 150 cm depth may indicate traces of the great floods of 1993/94,

255 11/26/2002 and 12/03/2003, and of 11/23/2016, respectively. These sedimentary layers can be dated to  
256 these periods by our model, reinforcing the age/depth model acquired for the Rhone core.

257 Amounts of sands are in general significantly higher in the Rhone core when compared to the  
258 Rhine, most probably due to (i) the specific hydro-sedimentary characteristics of the rivers, (ii) deposition  
259 environments and conditions, and (iii) the vicinity of the Rhone coring point to the water flow of the river  
260 (<5 m) when compared to the Rhine system (>50 m). Finally, the d90 versus d50 diagram (Figure S3)  
261 indicates sedimentary deposits mainly constituted after settling of uniform suspension, which most  
262 generally characterises the dominance of clay and silts in riverine sediments. These results underline that  
263 the two sediment cores studied are rather similar regarding the grain size of sedimentary deposits, and  
264 that particles deposited are generally rather similar over time.

### 265 **3.3 Organic matter parameters**

266 For both sediment cores, our results showed that TOC content ranged from 0.33% to 4.63% for  
267 the Rhine River and from 0.64% to 2.63% for the Rhone River (Table 1). TOC remained relatively constant  
268 with depth for the Rhone River but decreased for the Rhine River. The RC/TOC ratio ranged from 0.65 to  
269 0.76 for the Rhine River and from 0.74 to 0.91 for the Rhone River. Other parameters (S2, S3, S3CO and  
270 HI/OI) were higher for the Rhine River than for the Rhone River (Table 1).

### 271 **3.4. Environmental levels of PAEs and OPEs in Rhone and Rhine sediments**

272 Levels of PAEs and OPEs were both higher in Rhine sediment cores (Figures 3A and 3C) than in  
273 Rhone cores (Figures 3B and 3D), at *ca.* ten times higher for PAEs and four times higher for OPEs. Clearly,  
274 PAEs and OPEs concentrations increased over time from the first records to the most recent dates, with  
275 higher levels of PAEs (Figures 3C and 3D) than OPEs (Figures 3A and 3B), in both rivers. For both rivers,  
276 the trajectory of the plastic additive contamination is more obvious and linear for OPEs than for PAEs.  
277 Indeed, the concentrations of some PAEs can be seen to peak at times, then to decrease before rising  
278 again. However, for both categories of plastic additives, the first noticeable contamination appears in  
279 sediment dated around 1963, followed by a significant increase reported post-2000 (Figure 3).

### 280 **3.5. Relative abundances of PAEs and OPEs in sediments of the Rhone and Rhine rivers**

281 Interestingly, TPP was never detected in Rhone and Rhine sediment cores, and TiBP, TnBP, TDCP  
282 (OPEs) and DEP (PAE) were not detected in Rhone sediments (Figures 3E, 3F and 3G, Tables S5, S6, S7 and  
283 S8). By contrast, several additives were quantified in all layers of sediment cores: these include DiBP,  
284 DnBP, BBzP and DnOP in both rivers, DEHP, DEP, DMP (PAEs, Figures 3G and 3H), TDCP and TEHP (OPEs,  
285 Figures 3E and 3F) in the Rhine River, and TCPP in the Rhone River. In Rhone samples, EHDPP and DMP  
286 were quantified only in one or two middle layers, and TPhP only in upper layers. TPhP was also detected  
287 only in upper layers of Rhine sediments, with TnBP. Finally, some additives were measured in upper and  
288 middle layers: TiBP, TCEP, TCPP and EHDPP for the Rhine, and TCEP, TEHP and DEHP for the Rhone.

289 In Rhine sediment samples, TCPP and TEHP appeared to be the most abundant OPEs whereas  
290 DEHP followed by DiNP were the predominant PAEs. In the Rhone samples, TCPP and DEHP were also the  
291 most abundant OPE and PAE, respectively. Prior to 1963, only one OPE (TCPP) was detected in Rhone  
292 sediments, yet it was quantified only after 1963 in the Rhine, which presented TEHP, TDCP and TiBP in  
293 sediments before that date. For PAEs, DEHP appeared from 1909 in the Rhine, but was quantified only  
294 much later (1979) in the Rhone. Before these dates, DiBP, DnBP, BBzP and DNoP were reported in  
295 sediments of both rivers, and DMP and DEP additionally in the Rhine.

### 296 **3.6. Relationship between plastic additive levels, organic matter and granulometry**

297 Correlations between levels of each PAE, each OPE, total OPEs ( $\Sigma$ OPEs), total PAEs ( $\Sigma$ PAEs), with  
298 data related to OM (TOC, HI/OI, S2, S3 and S3CO) and granulometry (d10, d50 and d90) for the Rhine are  
299 quite similar to those for the Rhone (Figures 4 and S4). Data related to granulometry was not correlated  
300 with plastic additive levels. However, for both rivers, parameters related to OM were correlated with  
301 levels of OPEs and PAEs, while RC/TOC ratio was anti-correlated with those concentrations. Furthermore,  
302 concentrations of individual OPE and total OPEs presented stronger correlations with OM than did  
303 concentrations of individual PAE or total PAEs. Correlations between variables were stronger for the Rhine  
304 than for the Rhone. For the Rhine, TCPP, TDCP, EHDPP, TEHP and  $\Sigma$ OPEs, and DMP, BBzP, DEHP, DnOP and  
305  $\Sigma$ PAEs all showed strong positive correlations with all OM parameters ( $> 0.6$ ) except with RC/TOC. For the  
306 Rhone, only TCPP,  $\Sigma$ OPEs, DEHP and  $\Sigma$ PAEs presented quite strong positive correlations with all OM  
307 parameters ( $> 0.5$ ) except with RC/TOC.

## 308 **4. Discussion**

309 Historically, Western European River contamination trends of OPEs and PAEs has been poorly  
310 documented, with most of the existing studies omitting to date the sediment cores (Paluselli et al., 2018;  
311 Schmidt et al., 2020; Alkans et al., 2021; Nagorka and Koschorreck, 2020). Yet establishing the trajectories  
312 of plastic additives in sediment archives is of great importance for the reconstruction of environmental  
313 and human exposures to these contaminants over the last decades. Such approaches applied to plastics  
314 additives are scarcer and mechanisms involved in their sequestration are poorly documented. Plastic  
315 additives are hydrophobic substances that undoubtedly react with solid particles since they are largely  
316 encountered in the riverine, coastal and marine sedimentary compartments. In this study, the detection  
317 of OPEs and PAEs in sediment cores sampled in the Rhine and the Rhone rivers is reported since the  
318 earliest dates recorded (1860 and 1931, respectively). In these old years, OPEs and PAEs were probably  
319 not used as additives for plastics but in other applications. Also, a contamination in this study cannot be  
320 excluded. Apart from the temporal trends observed and discussed hereafter, relatively high levels during  
321 some short periods of time suggest periodic and localised historical pollution events. Data on additive  
322 production volume during the earlier years is not available at the scale of the studied watersheds, but van  
323 der Veen and de Boer (2012) demonstrated that OPEs have been employed worldwide for up to 150 years

324 and that PAEs have been used since the beginning of the 20<sup>th</sup> century. Today, they are in the class of  
325 synthetic chemicals with high production volumes and toxicological properties (Schechter et al. 2013).

326 **Temporal trends of OPE levels.** The contamination profiles of OPEs are similar for both rivers, with low  
327 concentrations before 1960, then increasing to finally reach the highest concentrations in the 2000s.  
328 These results are consistent with the history of OPEs, which were first introduced in the early 1900s with  
329 a rapid increase after the 1940s (USEPA, 1976). After early 21<sup>st</sup> century, the use of OPEs expanded  
330 significantly worldwide following the ban on polybrominated diphenyl ethers (Stapleton et al., 2012). As  
331 an example, in 2018, 1.05 million tons of OPEs were used globally (Z.C. Group, 2018). Cao et al. (2017)  
332 investigated the contamination of OPEs in dated sediment cores from Lake Michigan (USA) and reported  
333 concentrations of alkyl- (sum of TMP, TEP, TPrP, TiBP, TnBP, TBEP, and TEHP) and chlorinated (sum of  
334 TCEP, TCPP, and TDCP) OPEs from 1860 until the 2000s. However, existing studies reporting vertical  
335 distribution and historical contamination trends of OPEs in sediments have received little attention (Luo  
336 et al. 2023). Some studies reviewed by Wang et al. (2020) showed concentrations of OPEs in surface  
337 sediments sampled in Europe which are similar to those reported in this study. Indeed, mean levels of  
338  $\Sigma$ OPEs in several European rivers were measured at dozens to hundreds of  $\text{ng}\cdot\text{g}^{-1}$ , including rivers in Spain  
339 (Cristale et al., 2013), Austria (Martínez-Carballo et al., 2007), Germany (Stachel et al., 2005) and three  
340 European river basins (Adige, Evrotas and Sava) (Giulivo et al., 2017). In the coastal NW Mediterranean  
341 Sea, Alkan et al. (2021) reported  $\Sigma_9$ OPE concentrations from surface sediments sampled in 2018 in the  
342 Rhone River (Gulf of Lion) that ranged from 4 to 227  $\text{ng}\cdot\text{g}^{-1}$  dw (mean: 54  $\text{ng}\cdot\text{g}^{-1}$  dw).

343 In our study, TCPP was the dominant OPE in both rivers. A similar trend has been observed in other  
344 studies: Zhang et al. (2018) found that TCPP was one of the dominant OPEs in the microplastics collected  
345 from coastal beaches in China, accounting for 35.1%, and Ma et al. (2022) also found TCPP as the dominant  
346 OPE in sediments of the Dong Nai River (Vietnam), with an average contribution of 81%. Temporal trends  
347 observed by Cao et al. (2017) demonstrated that the recent increase in depositional flux to sediment is  
348 dominated by chlorinated OPEs, especially TCPP. TCPP levels reported in our study also suggest historical  
349 contamination, since the chemical was detected from 1931 in the Rhone River and from slightly later in  
350 the Rhine River, in 1963. This can be explained by the high production volume of TCPP and its common  
351 uses as a flame retardant to comply with flammability standards for rigid and spray polyurethane foam  
352 (building insulation), and for flexible polyurethane foam (furniture and automotive seating) (Babrauskas  
353 et al. 2012; van der Veen and de Boer, 2012). Due to the fact that TCPP is added but not chemically bonded  
354 to polymers, it can be released into the environment through volatilization, abrasion, and dissolution in  
355 addition to through direct contact with dust and surfaces (Rauert et al., 2014). Moreover, the  
356 concentrations of TEHP were dominant in the Rhine River compared to other OPEs and have continued  
357 to increase since the first record in 1860. TEHP, an alkyl-OPE, is usually added to paints, coatings and  
358 textiles (Chen and Ma, 2021; van der Veen and de Boer, 2012) but is not generally the most abundant OPE

359 in environmental samples. However, some studies have also measured high TEHP concentrations  
360 compared to other OPEs. For example, Sutton et al. (2019) reported higher TEHP concentrations in  
361 sediments of San Francisco Bay (median concentrations of  $8.2 \text{ ng.g}^{-1} \text{ dw}$ ) than other analysed phosphate  
362 flame retardants (TCrP, TPhP, TDCPP and TBEP). In the surface sediment samples of the Scheldt Estuary  
363 (Holland), TEHP ranged from 0.4 to  $3.3 \text{ ng.g}^{-1} \text{ dw}$  (Brandsma et al., 2015). TEHP was found to range from  
364  $0.620 \text{ ng.g}^{-1} \text{ dw}$  to  $7.90 \text{ ng.g}^{-1} \text{ dw}$  in the Dong Nai River System (Vietnam) (Ma et al., 2022), revealing levels  
365 that are comparable to the measurements reported in this paper. TEHP is hydrophobic with high logKow  
366 and may be strongly adsorbed by the sediments with high TOC content (Van der Veen and De Boer, 2012;  
367 Ma et al., 2022), which corroborates results from the Rhine River.

368 Finally, the pattern of OPEs was more diverse in Rhine sediments than in those of the Rhone. Despite the  
369 same order of magnitude of the concentrations of  $\Sigma\text{OPEs}$  compared to our study, Cao et al. (2017) found  
370 a more diverse profile of OPEs, with TCPP, TiBP, TnBP measured in sediments of their three studied lakes  
371 before the 1900s. Ma et al. (2022) demonstrated that human activities had a clear impact on the patterns  
372 and spatial distribution of OPEs in sediments. The nature of industrial activities that developed at the scale  
373 of the catchment upstream of the sampling points may thus explain the differences in diversity of OPEs  
374 between the Rhine and Rhone rivers.

375 **Temporal trends of PAE levels.** In 2009, worldwide PAE production stood at 6.2 million tons (He et al.,  
376 2019), of which a large amount is likely to be found in aquatic ecosystems. As is the case for OPEs,  
377 historical contamination of PAEs in sediments is still poorly documented. In this study, some PAEs from  
378 the first record (1860 and 1931, respectively) were measured at non-negligible concentrations in the  
379 Rhine and Rhone rivers, suggesting long-term contamination. Kang et al. (2016) showed historical  
380 contamination of some PAEs, dating DiBP and DnBP detected in Lake Chaohu sediments (China) to 1849.  
381 In addition to the historical contamination shown in our study, the unpredictable profile of  $\Sigma\text{PAE}$  levels in  
382 sediments over time with peaked concentrations at some dates, suggests localised and intermittent  
383 pollution of both rivers. What is more, the levels of PAEs remains higher than OPEs in both the Rhine and  
384 the Rhone. This is consistent with Alkan et al. (2021), who reported a maximum concentration of  $\Sigma\text{PAEs}$   
385 at  $766 \text{ ng.g}^{-1} \text{ dw}$  in surface sediments of the Rhone River (Gulf of Lion), while that of  $\Sigma\text{OPEs}$  reached  $227$   
386  $\text{ng.g}^{-1} \text{ dw}$ . Schmidt et al. (2021) also highlighted that PAEs ( $12\text{-}610 \text{ ng.g}^{-1} \text{ dw}$ ) concentrations were  
387 generally higher than OPEs ( $13\text{-}49 \text{ ng.g}^{-1} \text{ dw}$ ) in sediments collected from three different sampling stations  
388 in Marseille Bay (France).

389 Among all PAEs, DEHP is always present in the environment and has been dominant for decades in  
390 sediment samples in most cases (Bergé et al., 2013). Chen et al. (2018) detected DEHP in all sediment  
391 samples of the Love River (China), with concentrations between  $4.2$  and  $66.7 \text{ ng.g}^{-1} \text{ dw}$ , indicating that it  
392 is a common pollutant in the river's environment. Their results are close to those found for the Rhone  
393 River in this study, although they are about ten times higher in the Rhine River. Alkan et al. (2021) also

394 found that DEHP was the most abundant PAE, representing an average of 67% of the  $\Sigma$ PAEs. This  
395 occurrence is explained by the widespread applications of DEHP and by the fact that DEHP weakly binds  
396 with plastics. As a result, large amounts of DEHP may be being released into the environment directly  
397 from plastic materials and products (Chen et al., 2018). Despite existing alternatives to DEHP, such as  
398 diisononyl phthalate (DiNP) or diisodecyl phthalate (DiDP) (not studied in this work), this chemical remains  
399 present in various environmental matrices (Net et al. 2015). Considering that DEHP is highly sensitive to  
400 contamination during sampling, transport and analysis, it cannot be ruled out that our samples may be  
401 slightly contaminated, despite the precautions taken at all steps of the study and the estimated blank  
402 consideration. High DiBP and DnBP concentrations were also found in the Rhone and the Rhine rivers,  
403 which is in agreement with what has already been reported from the bottom to the surface in Lake Chaohu  
404 (China) core sediments (Kang et al., 2016). This is probably due to its high production and use around the  
405 world (Kang et al. 2016). Indeed, DnBP was primarily used in agricultural plastic film until being banned in  
406 2000, while DiBP is still widely used as a plasticizer and softener in the plastics industry. Due to this, DiBP  
407 constitutes one of the most common organic contaminants detected worldwide (Kang et al., 2016).  
408 Despite European regulations implemented since 2000 which ban products containing certain phthalates  
409 such as DEHP or DnBP, concentrations of PAEs found in aquatic environments remain alarming.

410 ***Influence of sediment grain size and organic matter parameters on PAEs and OPEs levels.*** The influence  
411 of sediment grain size and organic matter on the levels of plastic additives also remains poorly  
412 documented. However, it is expected that high specific surface area of grain sediment, most generally  
413 enriched in OM, induces higher adsorption of hydrophobic organic pollutants (Jaffé, 1991). Given that OM  
414 tends to adsorb on fine grains, a higher content of pollutants is commonly observed in this case (Chen et  
415 al., 2018; Ma et al., 2022). In addition to the different histories of urbanisation of the two rivers, the higher  
416 plastic additive concentrations found in the Rhine River may be explained by the river's higher proportion  
417 of fine sediments (Figure 2). However, in this study, no correlation between sediment grain size and plastic  
418 additive levels was highlighted by the Pearson correlations, excluding this last hypothesis and suggesting  
419 that the temporal distribution of OPEs and PAEs is not disrupted by the grain size. The grain size of  
420 archived particles is over all very similar and reflect close hydrodynamic conditions during the sedimentary  
421 particle settling. This suggests that the deposition of microplastic particles, if directly involved in plastics  
422 additive contents, was also driven from comparable processes and do not interfere on the temporal  
423 trends of plastic additives.

424 OM parameters were found in some cases to play an important role in the behaviour and the fate of  
425 plastic additives in the environment, even though the few existing reports in the literature put forward  
426 some controversial conclusions for both PAEs and OPEs. In the present study, the strong correlations  
427 observed in some cases between OPEs, PAEs contents and OM indicators suggest that OM and additives  
428 content sources are associated at certain periods, likely in relation with terrestrial runoff. This can be most



429 convincingly hypothesized in the case of the Rhine core, where OPE and PAE contents generally decreased  
430 with depth similarly to TOC contents. Nevertheless, such similar trends with depth between OPEs, PAEs  
431 and OM were not observed for the Rhone cores, where TOC contents are rather constant with depth  
432 unlike OPEs and PAEs, excluding the first hypothesis.

433 For PAEs, Xiang et al. (2019) concluded that the sorption of dibutyl phthalate (DBP) was inversely  
434 associated with soil particle sizes, and Xu and Li (2008) concluded that OM in sediments is essential to  
435 explain the DBP adsorption capacity. The correlation analysis performed by Chen et al. (2018) showed  
436 that grain size and OM may play a key role in DEHP distribution in the sediments during the dry season,  
437 whereas DEHP concentrations in the wet season may be principally affected by other environmental and  
438 hydrological conditions (transport, mixing and sedimentation mechanisms). Finally, Kang et al. (2016)  
439 found that the contents of  $\Sigma$ PAEs, as well as of individual PAEs (DMP, DEP, DiBP, DnBP, DEEP, DBEP, and  
440 DnOP) in sediment cores, were significantly positively correlated with the percentage of sand particles  
441 and, contrariwise, negatively correlated with the percentage of fine particles. They also highlighted the  
442 significantly positive relationship between TOC and the contents of  $\Sigma$ PAEs, as well as low-molecular-  
443 weight PAEs (DMP, DEP, DIBP, DnBP, DEEP).

444 Concerning the OPEs, Luo et al. (2020) found not only that the distribution pattern of  $\Sigma$ OPEs in different  
445 particle-size fractions is irregular and varies with the land-use types, but also that correlations between  
446 total OPEs or individual OPE concentrations versus TOC are weak. However, Ma et al. (2022) showed that  
447 the concentrations of TCPP and TEHP exhibit a significant moderate positive correlation with TOC, while  
448 TCPP showed no correlation with grain size, and TEHP presented a significant correlation with clay and  
449 silt, as well as showing a significant anti-correlation with sand. This corroborates the fact that OPEs with  
450 low water solubility such as TEHP, EHDPP and TPhP, TnBP and TiBP preferentially absorbed onto  
451 particulate OM (Martínez-Carballo et al., 2007). Compounds with higher logKow or higher logKoc values  
452 were more easily adsorbed by sediments, while OPEs with logKoc > 5 were almost completely associated  
453 with sediment particles (Cao et al., 2017; Ma et al., 2022). Other factors such as physicochemical  
454 properties, emission intensity and degradation may play a role in some instances (Ma et al., 2022). Herein,  
455 positive and significant correlations between plastic additive levels and OM parameters occur essentially  
456 with the pyrolyzed C (S2, S3, S3CO), while the negative correlations occur with the refractory C (RC/TOC).  
457 Accordingly, the sorption process appears to concern the labile fraction of sedimentary OM which exhibits  
458 chemical functional groups such as CH<sub>2</sub>, CH<sub>3</sub> (e.g methyl) for hydrogen and COH, CO (alcohol, ketone,  
459 ester) for oxygen. The additives studied here are potentially degradable in sediment like the rest of the  
460 organic compounds, with very probably different kinetics. It is important to note that the presence of  
461 contaminants such as OPEs can, in addition, induced a decrease on the diversity of the bacterial  
462 community (as number of microbial species) as has been demonstrated for OPEs in the coastal  
463 Mediterranean marine sediment (Castro-Jiménez et al., 2022). This modification could very likely

464 influence the degradation kinetics of natural organic matter. While some relationships between plastic  
465 additives and organic matter contents were highlighted in our study no information on the link with  
466 microplastic contents is currently available neither from our study nor the literature. In this context, the  
467 origin of plastics additives in sedimentary archives needs further investigation to be clearly identified, in  
468 particular the relations with microplastics contents.

## 469 **5. Conclusion**

470 Concentrations of  $\Sigma$ 9OPEs and  $\Sigma$ 7PAEs have increased continuously since temporal records  
471 reconstructed from sediment cores began to be kept, i.e. since 1860 for the Rhine River and 1930 for the  
472 Rhone River. Referring to the earliest comparative periods, the data acquired herein show elevated  
473 concentrations since the 1990s and even higher values since the 2000s. No correlation was seen between  
474 sediment grain size and plastic additive levels, while some parameters related to OM, such as TOC, were  
475 shown to correlate with OPEs and PAEs contents without disruption of temporal trends. The results of  
476 this study highlight the environmental changes that occurred during the last industrial era and reveal how  
477 the memory of riverine sediments provides a useful record for reporting environmental impacts related  
478 to human activities. This study also suggests that when incorporated into studies involving neural  
479 networks, our data may be helpful for establishing relationships between the levels of contamination  
480 observed in sedimentary archives and anthropogenic pressures. Finally, our results will contribute  
481 towards better protection of aquatic environments and the development of a management strategy  
482 concerning plastic additives.

## 483 **Acknowledgements**

484 The authors are grateful to the ANR TRAJECTOIRE project (ANR-19-CE3- 0009, 2020–2024) for financial  
485 support and warmly thank Francois Chabaux (Université de Strasbourg, Laboratoire d'HYdrologie et de  
486 GÉochimie de Strasbourg (LHyGeS), UMR 7517, École et Observatoire des Sciences de la Terre (EOST)),  
487 Laurent Schmitt and Dominique Babariotti (Université de Strasbourg, Laboratoire Image Ville  
488 Environnement (LIVE), UMR 7362, Faculté de Géographie et d'Aménagement), Hugo Lepage, Valérie  
489 Nicoulaud-Gouin, Franck Giner, David Mourier, Xavier Cagnat and Anne De Vismes (Institut de  
490 Radioprotection et de Sureté Nucléaire (IRSN)), François Baudin (ISTeP laboratory, Sorbonne Université  
491 for RE6 analyses).

## 492 **References**

- 493 Alkan, N., Alkan, A., Castro-Jiménez, J., Royer, F., Papillon, L., Ourgaud, M., Sempéré, R., 2021.  
494 Environmental occurrence of phthalate and organophosphate esters in sediments across the Gulf of  
495 Lion (NW Mediterranean Sea). *Sci. Total Environ.* 760, 143412.  
496 <https://doi.org/10.1016/j.scitotenv.2020.143412>
- 497 Appleby, P.G., 2008. Three decades of dating recent sediments by fallout radionuclides: a review. *The*  
498 *Holocene* 18, 83–93. <https://doi.org/10.1177/0959683607085598>
- 499 Arnaud, F., Piégay, H., Schmitt, L., Rollet, A.J., Ferrier, V., Béal, D. 2015. Historical geomorphic analysis  
500 (1932–2011) of a by-passed river reach in process-based restoration perspectives: The Old Rhine  
501 downstream of the Kembs diversion dam (France, Germany). *Geomorphology*. 236, 163–177.  
502 <https://doi.org/10.1016/j.geomorph.2015.02.009>

- 503 Babrauskas, V., Lucas, D., Eisenberg, D., Singla, V., Dedeo, M., Blum, A. 2012. Flame retardants in building  
504 insulation: a case for re-evaluating building codes. *Build Res Inf.* 40: 738–55. [https://doi.org/10.1080/](https://doi.org/10.1080/09613218.2012.744533)  
505 [09613218.2012.744533](https://doi.org/10.1080/09613218.2012.744533)
- 506 Baudin, F., Disnar, J.-R., Aboussou, A., Savignac, F. 2015. Guidelines for Rock–Eval analysis of recent marine  
507 sediments. *Organic Geochemistry.* 86, 71–80. <https://doi.org/10.1016/j.orggeochem.2015.06.009>
- 508 Bergé, A., Cladière, M., Gasperi, J., Coursimault, A., Tassin, B., Moilleron, R. 2013. Meta-analysis of  
509 environmental contamination by phthalates. *Environ Sci Pollut Res Int.* 20: 8057-76.  
510 <https://doi.org/10.1007/s11356-013-1982-5>
- 511 Blott, S., 2000. GRADISTAT Version 4.0. Surrey.
- 512 Blott, Simon J., and Kenneth Pye. 2001. Gradistat: A Grain Size Distribution and Statistics Package for  
513 the Analysis of Unconsolidated Sediments. *Earth Surface Processes and Landforms.* 26: 1237–  
514 1248. <https://doi.org/10.1002/esp.261>
- 515 Bouisset, P., Calmet, D. 1997. Hyper pure gamma-ray spectrometry applied to low-level environmental  
516 sample measurements. International Workshop on the Status of Measurement Techniques for the  
517 Identification of Nuclear Signatures, Geel, Belgium.
- 518 Brandsma, S.H., Leonards, P.E., Leslie, H.A., de Boer, J. 2015. Tracing organophosphorus and brominated  
519 flame retardants and plasticizers in an estuarine food web. *Sci. Total Environ.* 505: 22–31.
- 520 Bravard, J.P. 2010. Discontinuities in braided patterns: The River Rhone from Geneva to the Camargue  
521 delta before river training. *Geomorphology.* 117, 219–233.  
522 <https://doi.org/10.1016/j.geomorph.2009.01.020>
- 523 Cao, S., Zeng, X., Song, H., Li, H., Yu, Z., Sheng, G., Fuy, J. 2012. Levels and distributions of organophosphate  
524 flame retardants and plasticizers in sediment from Taihu Lake, China. *Environ. Toxicol. Chem.* 31,  
525 1478–1484. <https://doi.org/10.1002/etc.1872>
- 526 Cao, D., Guo, J., Wang, Y., Li, Z., Liang, K., Corcoran, M. B., et al. 2017. Organophosphate esters in sediment  
527 of the great lakes. *Environ. Sci. Technol.* 51 (3), 1441–1449. <https://doi.org/10.1021/acs.est.6b05484>
- 528 Carrie, J., Sanei, H., Stern, G. 2012. Standardisation of Rock–Eval pyrolysis for the analysis of recent  
529 sediments and soils. *Organic Geochemistry.* 46, 38–53.  
530 <https://doi.org/10.1016/j.orggeochem.2012.01.011>
- 531 Castro-Jiménez, J., Cuny, P., Militon, C. et al. 2022. Effective degradation of organophosphate ester flame  
532 retardants and plasticizers in coastal sediments under high urban pressure. *Sci Rep* 12, 20228.  
533 <https://doi.org/10.1038/s41598-022-24685-6>
- 534 Chen, C.F., Ju, Y.R., Lim, Y.C., Chang, J.H., Chen, C.W., Dong, C.D. 2018. Spatial and Temporal Distribution  
535 of Di-(2-ethylhexyl) Phthalate in Urban River Sediments. *Int J Environ Res Public Health.*  
536 11;15(10):2228. <https://doi.org/10.3390/ijerph15102228>
- 537 Chen, M. and Ma, W. 2021. A review on the occurrence of organophosphate flame retardants in the  
538 aquatic environment in China and implications for risk assessment. *Sci. Total Environ.* 783, 147064.  
539 <https://doi.org/10.1016/j.scitotenv.2021.147064>
- 540 Copard, Y., Di-Giovanni, C., Martaud, T., Albéric, P., & Olivier, J.E. 2006. Using Rock-Eval 6 pyrolysis for  
541 tracking fossil organic carbon in modern environments: implications for the roles of erosion and  
542 weathering. *Earth Surface Processes and Landforms.* 31, 135–153. <https://doi.org/10.1002/esp.1319>
- 543 Cristale, J., Vazquez, A. G., Barata, C., Lacorte, S. 2013. Priority and emerging flame retardants in rivers:  
544 Occurrence in water and sediment, *Daphnia magna* toxicity and risk assessment. *Environ. Int.* 59,  
545 232–243.
- 546 Dendievel, A.M., Mourier, B., Dabrin, A., Delile, H., Coynel, A., Gosset, A., Liber, Y., Berger, J.F., Bedell, J.P.  
547 2020. Metal pollution trajectories and mixture risk assessed by combining dated cores and subsurface  
548 sediments along a major European river (Rhône River, France). *Environ Int.* 144:106032.  
549 <https://doi.org/10.1016/j.envint.2020.106032>
- 550 Euzen C., Chabaux, F., Rixhon, G., Preusser, F., Eyrolle, F., Badarotti, D., Schmitt, L. 2023. Combining  
551 geochronological methods improves accuracy of young floodplain sediment dating, *Submitted*

- 552 Eyrolle F., Boyer P., Chaboche P.A., De Vismes A., Lepage H., Seignemartin G., Mourier B., et al. 2024.  
553 Temporal trajectories of artificial radiocaesium 137Cs in French rivers over the nuclear era  
554 reconstructed from sediment cores, Scientific reports, submitted.
- 555 Eyrolle F., Claval D., Gontier G. and Antonelli C. 2008. Radioactivity level in major French rivers:  
556 summary of monitoring chronicles acquired over the past thirty years and current status, Journal  
557 of Environmental Monitoring, 10. 800-811.
- 558 Fauvelle, V., Garel, M., Tamburini, C. et al. 2021. Organic additive release from plastic to seawater is lower  
559 under deep-sea conditions. Nat Commun 12, 4426. <https://doi.org/10.1038/s41467-021-24738-w>
- 560 Foucher, A., Chaboche, P.A., Sabatier, P., Evrard, O. 2021. A worldwide meta-analysis (1977–2020) of  
561 sediment core dating using fallout radionuclides including 137Cs and 210Pbxs, Earth Syst. Sci. Data, 13,  
562 4951–4966. <https://doi.org/10.5194/essd-13-4951-2021>, 2021
- 563 Giulivo, M., Capri, E., Kalogianni, E., Milacic, R., Majone, B., Ferrari, F., Eljarrat, E., Barceló, D. 2017.  
564 Occurrence of halogenated and organophosphate flame retardants in sediment and fish samples from  
565 three European river basins. Science of The Total Environment, 586: 782-791.  
566 <https://doi.org/10.1016/j.scitotenv.2017.02.056>
- 567 Goldberg, E.D. 1963. Geochronology with 210-Pb. Radioact. Dating 121–131.
- 568 Grosbois, C., Meybeck, M., Lestel, L., Lefèvre, I., Moatar, F., 2012. Severe and contrasted polymetallic  
569 contamination patterns (1900–2009) in the Loire River sediments (France). Sci. Total Environ. 435 436,  
570 290–305.
- 571 Guo, Y. and Kannan, K. 2012. Challenges Encountered in the Analysis of Phthalate Esters in Foodstuffs and  
572 Other Biological Matrices. Analytical and Bioanalytical Chemistry; 404, 2539–2554.  
573 <https://doi.org/10.1007/s00216-012-5999-2>
- 574 He, Y., Wang, Q., He, W., Xu, F., 2019. The occurrence, composition and partitioning of phthalate esters  
575 (PAEs) in the water-suspended particulate matter (SPM) system of Lake. Sci. Total Environ. 661, 285-  
576 293. <https://doi.org/10.1016/j.scitotenv.2019.01.161>
- 577 Heise, S., and Förstner, U. 2006. Risks from Historical Contaminated Sediments in the Rhine Basin. Water,  
578 air & soil pollution. 6, 625-636.
- 579 Jaffé, R. 1991. Fate of hydrophobic organic pollutants in the aquatic environment: A review,  
580 Environmental Pollution, 69: 237-257. [https://doi.org/10.1016/0269-7491\(91\)90147-O](https://doi.org/10.1016/0269-7491(91)90147-O)
- 581 Joerss, H., Schramm, T.R., Sun, L., Guo, C., Tang, J., Ebinghaus R. 2020. Per- and polyfluoroalkyl substances  
582 in Chinese and German river water - Point source- and country-specific fingerprints including unknown  
583 precursors. Environ Pollut. 267:115567. <https://doi.org/10.1016/j.envpol.2020.115567>
- 584 Kang, L., Wang, Q.M., He, Q.S. et al. 2016. Current status and historical variations of phthalate ester (PAE)  
585 contamination in the sediments from a large Chinese lake (Lake Chaohu). Environ Sci Pollut Res. 23,  
586 10393–10405. <https://doi.org/10.1007/s11356-015-5173-4>
- 587 Lefèvre, O., Bouisset, P., Germain, P., Barker, E., Kerlau, G., Cagnat, X. 2003. Self-absorption correction  
588 factor applied to 129I measurement by direct gamma-X spectrometry for Fucus serratus samples.  
589 Nuclear Instruments and Methods in Physics Research A. 506 (1-2), 173–185.
- 590 Luo, Q., Wu, Z., & Gu, L. 2020. Distribution Pattern of Organophosphate Esters in Particle-Size Fractions  
591 of Urban Topsoils Under Different Land-Use Types and Its Relationship to Organic Carbon Content.  
592 Archives of Environmental Contamination and Toxicology. 79, 208–218.  
593 <https://doi.org/10.1007/s00244-020-00747-6>
- 594 Luo, Q., Wang, C., Gu, L., Wu, Z. and Li, Y. 2023. Temporal trends of organophosphate esters in a sediment  
595 core from the tidal flat of Liao River estuary, Northeast China. Front. Mar. Sci. 10: 1160371.  
596 <https://doi.org/10.3389/fmars.2023.1160371>
- 597 Ma, Y., Saito, Y., Ta, T.K.O., Li, Y., Yao, Q., Yang, C., Nguyen, V. L., Gugliotta, M., Wang, Z., Chen, L. 2022.  
598 Distribution of organophosphate esters influenced by human activities and fluvial-tidal interactions in  
599 the Dong Nai River System, Vietnam. Science of The Total Environment. 812, 152649.
- 600 Martínez-Carballo, E.; Gonzalez-Barreiro, C.; Sitka, A.; Scharf, S.; Gans, O. 2007. Determination of selected  
601 organophosphate esters in the aquatic environment of Austria. Sci. Total Environ. 388 (1–3), 290–299.

- 602 Middelkoop, H. 2000. Heavy-metal pollution of the river Rhine and Meuse floodplains in the Netherlands.  
603 Netherlands Journal of Geosciences, 79, 411-427. <https://doi.org/10.1007/S0016774600021910>
- 604 Mourier, B., Desmet, M., Van Metre, P.C., Mahler, B.J., Perrodin, Y., Roux, G., Bedell, J.P., Lefèvre, I., Babut,  
605 M. 2014. Historical records, sources, and spatial trends of PCBs along the Rhone River (France). *Sci.*  
606 *Total Environ.* 476–477, 568–576. <https://doi.org/10.1016/j.scitotenv.2014.01.026>
- 607 Mourier, B., Labadie, P., Desmet, M., Grosbois, C., Raux J., Debret M., Copard Y., Pardon P., Budzinski, H.,  
608 Babut, M. 2019. Combined spatial and retrospective analysis of fluoroalkyl chemicals in fluvial  
609 sediments reveal changes in levels and patterns over the last 40 years. *Environ Pollut.* 253: 1117-1125.  
610 <https://doi.org/10.1016/j.envpol.2019.07.079>
- 611 Munoz, G., Giraudel, J.L., Botta, F., Lestremau, F., Dévier, M.H., Budzinski, H., Labadie, P. 2015. Spatial  
612 distribution and partitioning behavior of selected poly- and perfluoroalkyl substances in freshwater  
613 ecosystems: a French nationwide survey. *Sci Total Environ.* 517: 48-56.  
614 <https://doi.org/10.1016/j.scitotenv.2015.02.043>
- 615 Nagorka, R., Koschorreck, J. 2020. Trends for plasticizers in German freshwater environments - Evidence  
616 for the substitution of DEHP with emerging phthalate and non-phthalate alternatives. *Environ Pollut.*  
617 262:114237. <https://doi.org/10.1016/j.envpol.2020.114237>
- 618 Net, S., Sempéré, R., Delmont, A., Paluselli, A., Ouddane, B. 2015. Occurrence, fate and behavior and  
619 ecotoxicological state of phthalates in different environmental matrices. *Environ. Sci. Technol.* 49,  
620 4019–4035. <https://doi.org/10.1021/es505233b>
- 621 Olivier, J.M., Dole-Olivier, M.J., Amoros, C., Carrel, G., Malard, F., Lamouroux, N., Bravard, J.P. 2009.  
622 Chapter 7 - The Rhône River Basin, in: Tockner, K., Uehlinger, U., Robinson, C.T. (Eds), *Rivers of Europe*,  
623 Academic Press. 247-295. <https://doi.org/10.1016/B978-0-12-369449-2.00007-2>
- 624 Olivier, J.M., Carrel, G., Lamouroux, N., Dole-Olivier, M.J., Malard, F., Bravard, J.P., Piégay, H., Castella, E.,  
625 Barthélemy, C., 2022. Chapter 7 - The Rhone River Basin, in: Tockner, K., Zarfl, C., Robinson, C.T. (Eds.),  
626 *Rivers of Europe (Second Edition)*. Elsevier. 391–451.
- 627 Paluselli, A., Aminot, Y., Galgani, F., Net, S., Sempéré, R., Occurrence of phthalate acid  
628 esters (PAEs) in the northwestern Mediterranean Sea and the Rhone River, *Progress in Oceanography*  
629 (2017), <http://dx.doi.org/10.1016/j.pocean.2017.06.002>
- 630 Paluselli, A., Fauvelle, V., Schmidt, N., Galgani, F., Net, S., Sempéré, R. 2018. Distribution of phthalates in  
631 Marseille Bay (NW Mediterranean Sea). *Sci. Total Environ.* 621, 578–587.  
632 <https://doi.org/10.1016/j.scitotenv.2017.11.306>
- 633 Provansal M., Villiet J., Eyrolle F., Raccasi G., Gurriaran R. and Antonelli C. 2010. High-resolution  
634 evaluation of recent bank accretion rate of the managed Rhone: A case study by multi-proxy approach,  
635 *Geomorphology.* 117, 287-297.
- 636 Rauert, C., Lazarov, B., Harrad, S., Covaci, A., Stranger, M. 2014. A review of chamber experiments for  
637 determining specific emission rates and investigating migration pathways of flame retardants. *Atmos*  
638 *Environ.* 82: 44–55. <https://doi.org/10.1016/j.atmosenv.2013.10.003>
- 639 Riquier, J., 2015. Réponses hydrosédimentaires de chenaux latéraux restaurés du Rhône français.  
640 Université de Lyon, France.
- 641 Schecter, A., Lorber, M., Guo, Y., Wu, Q., Yun, H.S., Kannan, K., Hommel, M., Imran, N.S.L., Cheng, D.H.,  
642 Colacino, J.A., Birnbaum, L.S. 2013. Phthalate concentrations and dietary exposure from food  
643 purchased in New York state. *Environ. Health Perspect.* 121: 473–479.
- 644 Schmidt, N., Castro-Jimenez, J., Fauvelle, V. and Sempéré R. 2020. Plastic organic additives in the Rhone  
645 River (France) surface waters – a one-year monitoring study. *Env. Pol.*, 257, 113637,  
646 <https://doi.org/10.1016/j.envpol.2019.113637>
- 647 Schmidt, N., Castro-Jiménez, J., Fauvelle, V., Sempéré, R. 2018. Zooplankton and Plastic Additives—  
648 Insights into the Chemical Pollution of the Low-Trophic Level of the Mediterranean Marine Food Web.  
649 *Proceedings of the International Conference on Microplastic Pollution in the Mediterranean Sea.*  
650 Springer Water. Springer, Cham. [https://doi.org/10.1007/978-3-319-71279-6\\_17](https://doi.org/10.1007/978-3-319-71279-6_17)
- 651 Schmidt, N., Castro-Jimenez, J., Oursel, B. and Sempéré, R. 2021. Phthalates and Organophosphate Esters  
652 in Surface Water, Sediments and Zooplankton of the NW Mediterranean Sea: Exploring Links with

- 653 Microplastic Abundance and Accumulation in the Marine Food Web. *Environmental Pollution*, 272,  
654 115970. <https://doi.org/10.1016/j.envpol.2020.115970>
- 655 Schmitt, L. 2001. Typologie hydro-géomorphologique fonctionnelle de cours d'eau : Recherche  
656 méthodologique appliquée aux systèmes fluviaux d'Alsace (These de doctorat). Université Louis  
657 Pasteur (Strasbourg) (1971-2008).
- 658 Seignemartin, G., Mourier, B., Riquier, J., Winiarski, T., Piégay, H. 2023. Dike fields as drivers and witnesses  
659 of twentieth-century hydrosedimentary changes in a highly engineered river (Rhône River, France).  
660 *Geomorphology*. 431, 108689. <https://doi.org/10.1016/j.geomorph.2023.108689>
- 661 Sempéré, R., Charrière, B., van Wambeke, F., Cauwet, G. 2000. Carbon inputs of the Rhône River to the  
662 Mediterranean Sea: Biogeochemical implications. *Global Biogeochemical Cycles*, 14: 669-681.  
663 <https://doi.org/10.1029/1999GB900069>
- 664 Stachel, B., Jantzen, E., Knoth, W., Kruger, F., Lepom, P., Oetken, M., Reincke, H., Sawal, G., Schwartz, R.,  
665 Uhlig, S. 2005. The Elbe flood in August 2002 - Organic contaminants in sediment samples taken after  
666 the flood event. *J. Environ. Sci. Health, Part A: Toxic/ Hazard. Subst. Environ. Eng.* 40 (2), 265-287.
- 667 Stapleton, H. M., Sharma, S., Getzinger, G., Ferguson, P.L., Gabriel, M., Webster, T.F., Blum, A. 2012. Novel  
668 and high volume use flame retardants in US couches reflective of the 2005 pentaBDE phase out.  
669 *Environ. Sci. Technol.* 46 (24), 13432-13439.
- 670 Statista Research Department, Jun 12, 2023. [https://www.statista.com/statistics/282732/global-  
671 production-of-plastics-since-1950/](https://www.statista.com/statistics/282732/global-production-of-plastics-since-1950/)
- 672 Sutton, R., Chen, D., Sun, J., Greig, D.J., Wu, Y. 2019. Characterization of brominated, chlorinated, and  
673 phosphate flame retardants in San Francisco Bay, an urban estuary. *Science of The Total Environment*.  
674 652, 212-223. <https://doi.org/10.1016/j.scitotenv.2018.10.096>
- 675 Tena, A., Piégay, H., Seignemartin, G., Barra, A., Berger, J.F., Mourier, B., Winiarski, T., 2020. Cumulative  
676 effects of channel correction and regulation on floodplain terrestrialisation patterns and connectivity.  
677 *Geomorphology* 354, 107034. <https://doi.org/10.1016/j.geomorph.2020.107034>
- 678 USEPA. 1986. EPA Regulation 40 CFR part 136 (appendix b) appendix b to part 136 d definition and  
679 procedure for the determination of the method detection limited revision 1.11 (US Environmental  
680 Protection Agency (EPA). Available at: <http://www.ecfr.gov/>(Accessed 5 March 2013).
- 681 van der Veen, I. and de Boer, J. 2012. Phosphorus flame retardants: properties, production environmental  
682 occurrence, toxicity and analysis. *Chemosphere* 88, 1119-1153.  
683 <https://doi.org/10.1016/j.chemosphere.2012.03.067>
- 684 Wang, X., Zhu, Q.Q., Yan, X.T., Wang, Y.W., Liao, C.Y., and Jiang, G.B. 2020. A review of organophosphate  
685 flame retardants and plasticizers in the environment: Analysis, occurrence and risk assessment. *Sci.*  
686 *Total Environ.* 731, 139071. <https://www.10.1016/j.scitotenv.2020.139071>
- 687 Wei, G.L., Li, D.Q., Zhuo, M.N., Liao, Y.S., Xie, Z.Y., Guo, T.L., Li, J.J., Zhang, S.Y., Liang, Z.Q. 2015.  
688 Organophosphorus flame retardants and plasticizers: sources, occurrence, toxicity and human  
689 exposure. *Environ. Pollut.* 196, 29-46. <https://doi.org/10.1016/j.envpol.2014.09.012>
- 690 Xiang, L., Wang, X.D., Chen, X.H. Mo, C.H., Li, Y.W. Li, H., Cai, Q.Y., Zhou, D.M., Wong, M.H., and Li  
691 Q.X. 2019. Sorption Mechanism, Kinetics, and Isotherms of Di-n-butyl Phthalate to Different Soil  
692 Particle-Size Fractions. *Journal of Agricultural and Food Chemistry* 67: 4734-4745.  
693 <https://www.10.1021/acs.jafc.8b0635>
- 694 Xu, X.R. and Li, X.Y. 2008. Adsorption behaviour of dibutyl phthalate on marine sediments. *Mar Pollut*  
695 *Bull.* 57:403-8. <https://doi.org/10.1016/j.marpolbul.2008.01.023>
- 696 Yang, J., Zhao, Y., Li, M., Du, M., Li, X., Li, Y., 2019. A review of a class of emerging contaminants: the  
697 classification, distribution, intensity of consumption, synthesis routes, environmental effects and  
698 expectation of pollution abatement to organophosphate flame retardants (OPFRs). *Int. J. Mol. Sci.* 20,  
699 1-38. <https://doi.org/10.3390/ijms20122874>
- 700 Z.C. Group, In-depth Investigation and Investment Prospect Analysis Report of China's Flame Retardant  
701 Market in 2014-2018, Zhiyan Consulting Group, 2018.

702 Zhang, H., Zhou, Q., Xie, Z., Zhou, Y., Tu, C., Fu, C., Mi, W., Ebinghaus, R., Christie, P., Luo, Y. 2018.  
703 Occurrences of organophosphorus esters and phthalates in the microplastics from the coastal beaches  
704 in north China. *Sci Total Environ.* 616-617:1505-1512. <https://doi.org/10.1016/j.scitotenv.2017.10.163>

Journal Pre-proof

**Table 1.** Proportion of total organic carbon in studied sediment core samples (TOC%), ratio of residual carbon to total organic carbon (RC/TOC), hydrocarbons (S2, S3, S3CO) and the ratio of the index of hydrogens to the index of oxygens (HI/OI) for the Rhone and the Rhine sediment core samples.

Rhone							Rhine						
Sample	TOC(%)	RC/TOC	S2	S3CO	S3	HI/OI	Sample	TOC(%)	RC/TOC	S2	S3CO	S3	HI/OI
2020	1.01	0.79	1.62	0.34	1.79	1.08	2020.4	4.63	0.65	15.06	2.52	8.6	1.95
2017	2.63	0.74	5.86	1.06	4.62	1.48	2017.1	4.3	0.68	12.09	1.87	7.98	1.75
2013.9	1.29	0.79	2.06	0.53	2.15	1.1	2013.7	3.25	0.7	8.22	1.57	6.63	1.44
2011.2	1.47	0.8	2.25	0.57	2.35	1.1	2010.3	3.07	0.7	7.64	1.46	6.35	1.4
2006.5	0.94	0.83	1.06	0.29	1.64	0.78	2007	3.22	0.71	7.58	1.54	7.27	1.23
2002.4	0.64	0.82	0.76	0.21	1.29	0.71	2002.3	3.14	0.71	7.26	1.54	6.79	1.25
1995.6	0.99	0.82	1.17	0.32	1.9	0.75	1996.1	2.74	0.71	6.47	1.39	5.81	1.29
1989.1	1.45	0.83	1.79	0.45	2.36	0.9	1989.4	2.44	0.72	5.46	1.15	5.26	1.22
1979.2	0.89	0.83	0.98	0.26	1.64	0.73	1978.3	1.91	0.72	4.34	0.93	4.44	1.15
1962.6	1.29	0.91	0.84	0.21	1.36	0.76	1963	1.63	0.72	3.61	0.8	3.65	1.16
1959.5	0.8	0.88	0.62	0.15	1.09	0.71	1960.3	1.41	0.74	2.83	0.76	3.31	1
1957.8	0.59	0.85	0.52	0.15	1.02	0.63	1957.3	1.03	0.74	2	0.46	2.42	0.99
1956.2	0.7	0.89	0.47	0.11	0.99	0.6	1947.5	0.62	0.71	1.37	0.28	1.4	1.16
1946	0.76	0.86	0.73	0.18	1.16	0.77	1940	0.53	0.75	0.95	0.25	1.28	0.88
1938.1	1.18	0.9	0.87	0.18	1.15	0.93	1909.1	0.74	0.76	1.34	0.35	1.73	0.92
1931.8	0.75	0.83	0.87	0.21	1.17	0.9	1897.9	0.33	0.73	0.72	0.15	0.59	1.4
							1860	0.45	0.76	0.77	0.25	0.91	0.96



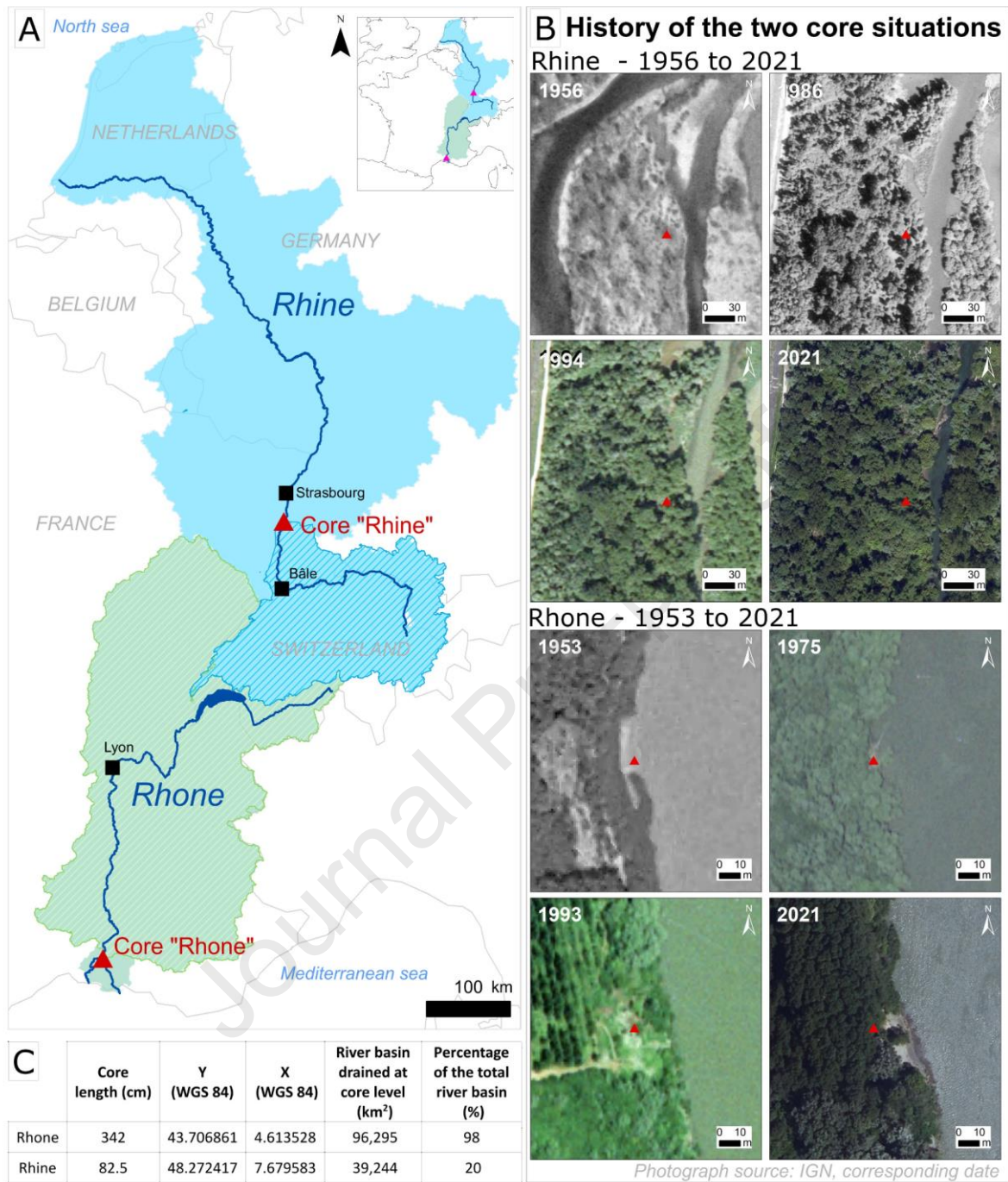


**Figure 1.** **A.** Location of Rhine and Rhone cores with associated drained watersheds (shaded); **B.** Historical evolution of coring sites from aerial photographic archives (photograph source: IGN); **C.** Characteristics of the cores.

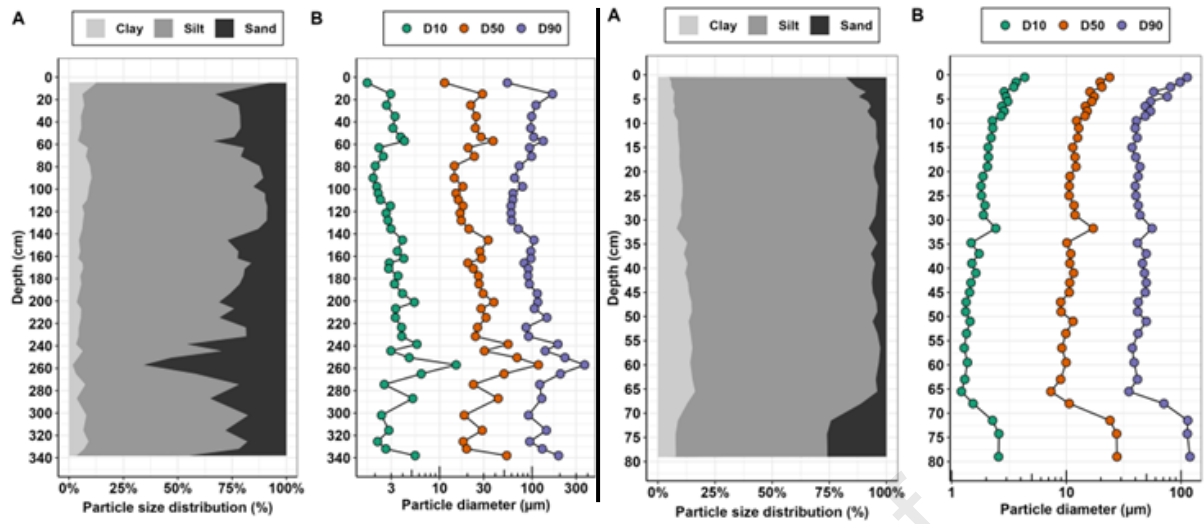


**Figure 2.** Particle size distribution (A) and diameter (B) of the sediment core samples of the Rhone River (left) and Rhine River (right).

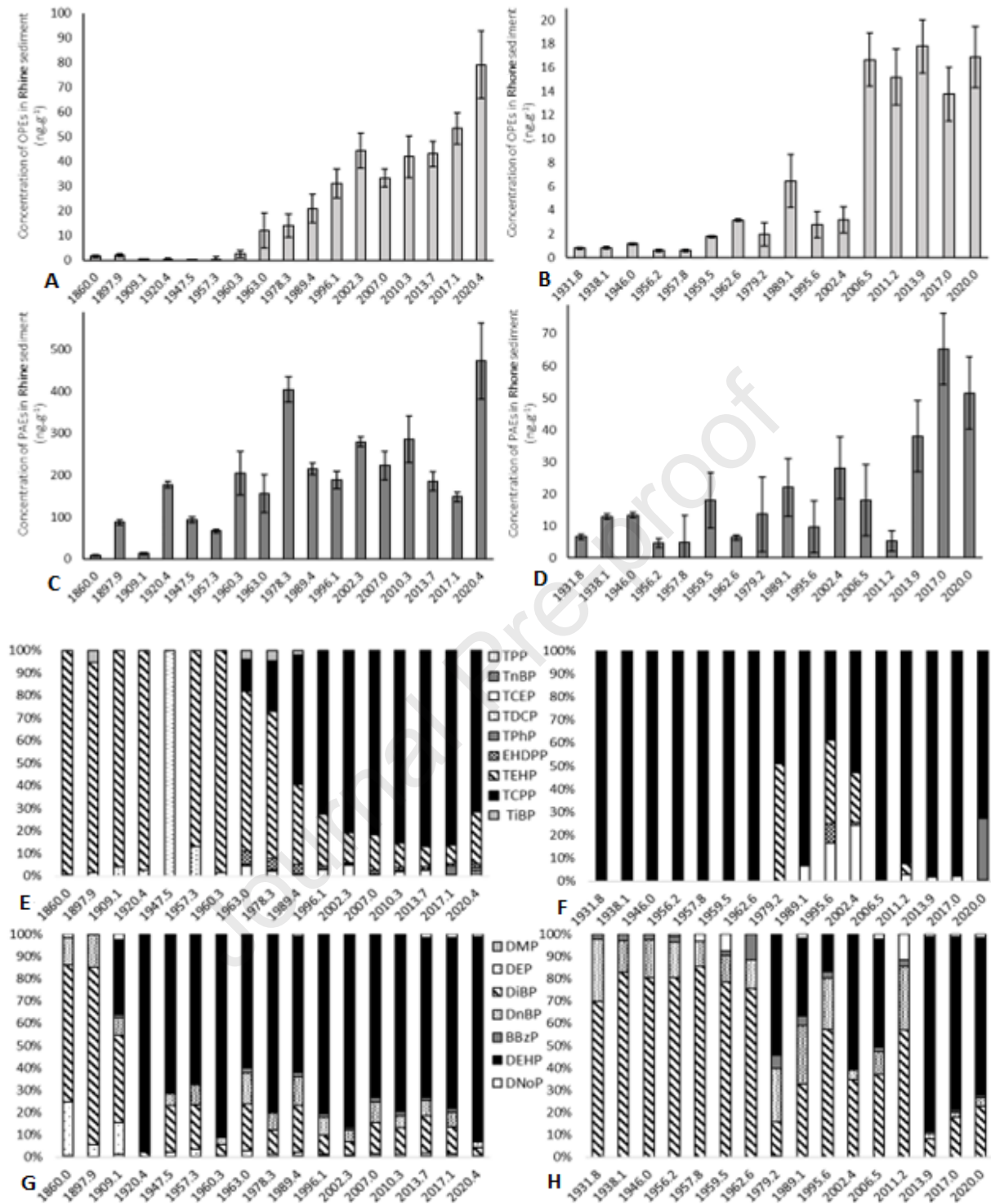


**Figure 3.** Concentrations (ng.g<sup>-1</sup> dw) of OPEs (A and B) and PAEs (C and D), and relative abundances of individual OPE (E and F) and PAE (G and H) measured in sediment core samples of the Rhine River (A and C) and the Rhone River (B and D).

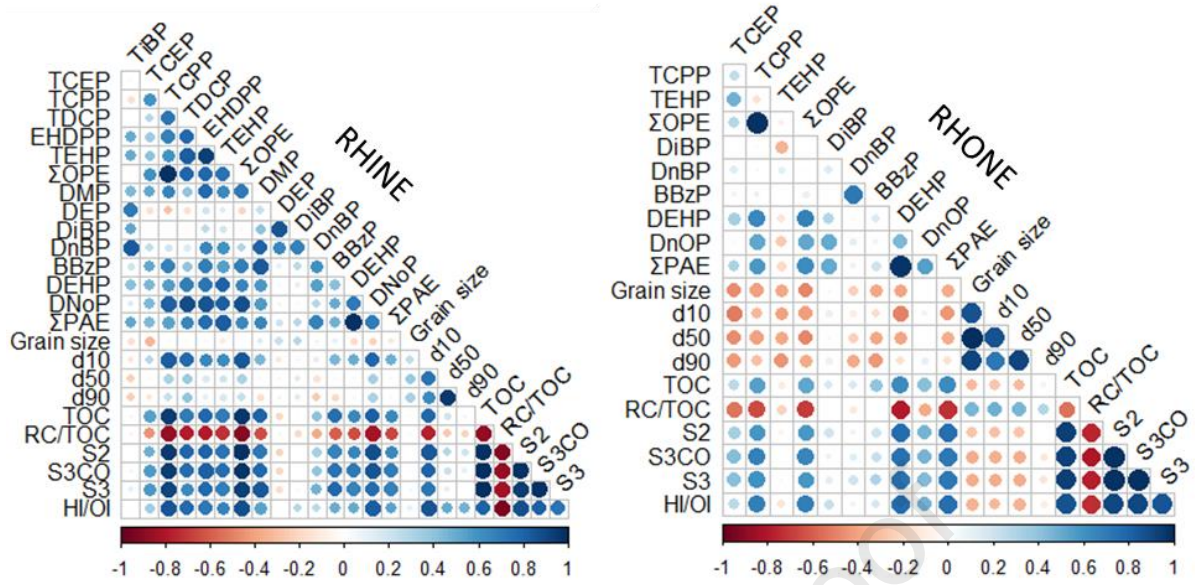


**Figure 4.** Pearson correlations of the levels of each PAE, each OPE, grain size, d10, d50, d90 and all organic matter factors (TOC, RC/TOC, S2, S3, S3CO and HI/OI ratio) of sediment core samples of Rhine and Rhone rivers. The red circles correspond to anti-correlations while the blue ones correspond to correlations. The larger the diameter of the circles, the stronger the correlations.

### Highlights

- Phthalates (PAEs) appeared in riverine sediments before the 1900s
- Organophosphate ester (OPE) sediment levels increased continuously from the 1900s
- Higher concentrations of PAEs than OPEs were observed in sediments of both rivers
- Tris(2-chloroisopropyl) phosphate (TCPP) was the dominant OPE in sediments
- Di(2-ethylhexyl) phthalate (DEHP) was the dominant PAE in sediments
- A positive correlation was found between plastic additive level and organic matter

**Declaration of interests**

The authors declare that they have no known competing financial interests or personal relationships that could have appeared to influence the work reported in this paper.

The authors declare the following financial interests/personal relationships which may be considered as potential competing interests:

Journal Pre-proof